Available online at www.eccomasproceedia.org
Eccomas Proceedia COMPDYN (2023) 4206-4216

ECCOMAS
Proceedia

COMPDYN 2023
9th ECCOMAS Thematic Conference on
Computational Methods in Structural Dynamics and Earthquake Engineering
M. Papadrakakis, M. Fragiadakis (eds.)
Athens, Greece, 12-14 June 2023

DYNAMIC RESPONSE OF TREES SUBJECT TO A LANDSLIDE-INDUCED AIR BLAST: IMPLICATIONS FOR AIR BLAST RISK ASSESSMENTS

Yu Zhuang[1,2*], Perry Bartelt[1,3], Aiguo Xing[2], Alexander Bast[1,3]

[1] WSL Institute for Snow and Avalanche Research SLF
Flüelastrasse 11, 7260 Davos Dorf, Switzerland
e-mail: Yu.Zhuang@slf.ch, bartelt@slf.ch, alexander.bast@slf.ch

[2] State Key Laboratory of Ocean Engineering, Shanghai Jiao Tong University
Shanghai, 200240, PR China
Yu.Zhuang@slf.ch, xingaiguo@sjtu.edu.cn

[2] Climate Change, Extremes and Natural Hazards in Alpine Regions Research Center CERC
Flüelastrasse 11, 7260 Davos Dorf, Switzerland
bartelt@slf.ch, alexander.bast@slf.ch

Abstract

Large landslides are known to generate powerful air blasts capable of causing damage far beyond the landslide runout. In many cases, observations of tree destruction are the only evidence to quantify the air blast danger. In this study, we proposed an approach to assess the air blast power using the tree breakage information, including the eigenfrequency prediction, tree motion calculation and breakage conditions. The tree is modelled as a flexible beam with elastic support at the tree base. Large tree deflection is accounted for when calculating the air blast loading and two failure modes (bending and overturning) are defined. Modelling results illustrated that tree eigenfrequency is always close to the air blast frequency, leading to a dynamic magnification for tree deformation. This magnification effect is greatly influential in a weak air blast case, but the large tree inclination resulting from strong air blast loading would weaken the effect. Additionally, both failure modes are likely to occur and the exact failure mode of trees depends heavily on their bending and anchorage resistance. Therefore, further measurements need to be conducted on the biometric and mechanical characteristics of trees, which will improve the accuracy of air blast hazard assessment.

Keywords: Landslide-induced air blast, Tree eigenfrequency, Dynamic response, Tree breakage.

ISSN:2623-3347
Peer-review under responsibility of the organizing committee of COMPDYN 2023.
doi: 10.7712/120123.10713.20982

1 INTRODUCTION

Long runout landslides are characterized by their high mobility, long moving distance and possible chain disasters [1]. A moving landslide with a large volume can generate powerful air blasts that are capable of breaking trees and even flattening buildings [2,3]. In recent years, destructive air blasts that caused mass casualties and damages are frequently recorded worldwide [4-6]. Understanding their destructive force is of great importance for landslide disaster prevention in mountainous regions.

Monitoring equipment has been proved to be a great approach to determine the air blast dynamics [7,8]. However, most cases occurred in the mountainous regions without a warning, and no monitoring equipment was settled in advance [9]. Therefore, very few air blast cases were measured in history. The occurrence of air blasts can be identified through the suspended powder cloud and geological evidence. In many cases, observations of tree breakage are the only data to quantify the air blast power [10]. Geologists can assess the air blast hazard using forest destruction and tree breakage information [11,12]. Snapped stems and uprooted/overturned trees outlined the impact area of air blasts and their falling direction could indicate the primary movement of the landslide. Any information on forest damage is valuable to help evaluate the air blast hazard.

The problem with using information of tree breakage for air blast risk assessment is that a simple relationship between air blast pressure and tree failure is hard to establish. Bending and overturning are two common tree failure modes caused by strong winds. Bending failure occurs when the bending stress exerted by the air blast exceeds the wood strength [13, 14], while the uprooting will occur when the applied torque overcomes the anchorage resistance [15-16]. Occurrence of the specific failure mode depends heavily on both the tree strength and air blast loading. Accounting for the minor destructive force of air blasts relative to the landslide, though long recognized that flowing sliding mass can easily break trees, tree destruction results from air blast loading has received less attention [17]. Existing models quantifying the air blast-induced tree breakage are mostly static [11] or proposed based on the small-deflection theory [10]. These approaches help the rapid evaluation of air blast power, but further research is needed to focus on the dynamic response of trees subjected to a strong wind loading.

Here we developed a simple mechanical model to calculate the natural frequency of trees and their dynamic response subject to an air blast loading. The tree is assumed as a multi-degree-of-freedom beam with variable diameters and the impacts of large deflection and root anchorage are accounted for. Furthermore, both bending and overturning failure modes are involved in the proposed model. Our work is expected to provide insights into the destructive force of landslide-induced air blasts and offers an applicable method for air blast hazard assessment.

2 MODEL DESCRIPTION

Landslide-induced air blasts are known of short duration, large impact area and can reach an extremely high velocity [7, 18]. The impact of this impulse wave on trees is similar to strong wind gusts, producing large bending stress/moments in the stem and root system, forcing trees to get deformation. To describe the dynamic response and failure of trees subject to the air blast loading, we proposed a dynamic tree-swaying model that accounts for the large tree deflection, including the eigenfrequency prediction method, tree motion equations and the breakage conditions.

2.1 Eigenfrequency prediction

The tree is modelled as a flexible cantilever beam that is hinged at the ground surface using elastic support (Fig. 1). Considering the decreasing diameter of stems and crown from bottom to top, the beam diameter is assumed to linearly decrease with height. Additionally, the tilt of tree base in response to the moment is described by the anchorage stiffness (K) of the root system [19]. In the eigenfrequency prediction model, the tree beam is split into two segments with a splitting point at the crown base. We assume that the tree crown shows minor impacts on elastic modulus and is accounted for through the crown mass.

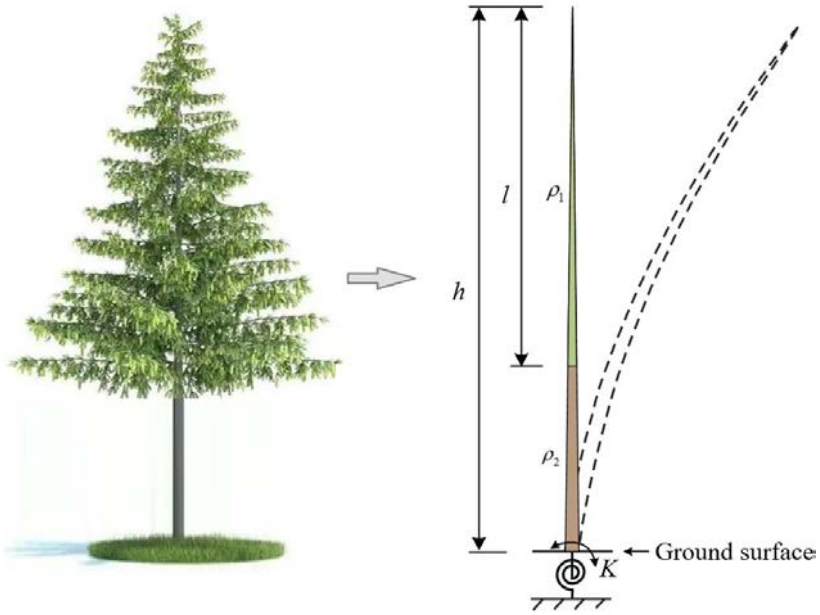

Fig. 1 Diagrammatic sketch of the eigenfrequency prediction model.

The governing equation for the dynamic bending of a nonuniform Euler-Bernoulli beam can be written as [20]:

$$z^2\frac{\partial^4 u}{\partial z^4}+8z\frac{\partial^3 u}{\partial z^3}+12\frac{\partial^2 u}{\partial z^2}-\frac{16\rho\omega^2 u}{E\mu^2}=0 \tag{1}$$

where u is the tree displacement, ρ is the material density, ω is the eigenfrequency, E is the elastic modulus, z is the position variable along the beam length. The original point (z=0) is set at the treetop to simplify the calculation, so that the beam diameter $d(z)$ at position z can be easily described by a gradient coefficient (μ): $d(z)=\mu z$. The general solution of Eq. 2 can be expressed as:

$$u(z)=\frac{1}{z}\left[A_1J_2(2\sqrt{\lambda z})+A_2Y_2(2\sqrt{\lambda z})+A_3J_2(2i\sqrt{\lambda z})+A_4Y_2(2i\sqrt{\lambda z})\right] \tag{2}$$

where $\lambda=\sqrt{\frac{16\rho\omega^2}{E\mu^2}}$, J_2 and Y_2 represent the Bessel functions of the first and send kind, respectively. A_1-A_4 are coefficients that need to be calculated according to the boundary and continuity conditions.

According to Eq. (2), the deformation of the upper crown segment and the lower trunk segment can be similarly expressed as:

$$u_1(z)=\frac{1}{z}\left[A_1J_2\left(2\sqrt{\lambda_1 z}\right)+A_2Y_2\left(2\sqrt{\lambda_1 z}\right)+A_3J_2\left(2i\sqrt{\lambda_1 z}\right)+A_4Y_2\left(2i\sqrt{\lambda_1 z}\right)\right] \quad 0\leqslant z<l \tag{3}$$

$$u_2(z)=\frac{1}{z}\left[B_1J_2\left(2\sqrt{\lambda_2 z}\right)+B_2Y_2\left(2\sqrt{\lambda_2 z}\right)+B_3J_2\left(2i\sqrt{\lambda_2 z}\right)+B_4Y_2\left(2i\sqrt{\lambda_2 z}\right)\right] \quad l\leqslant z\leqslant h \quad (4)$$

where l represents the crown length, h is the tree height, $\lambda_1=\sqrt{\frac{16\rho_1\omega^2}{E\mu^2}}$ and $\lambda_2=\sqrt{\frac{16\rho_2\omega^2}{E\mu^2}}$ are the single-valued function of eigenfrequency, ρ_2 is the wood density, ρ_1 is the equivalent density attributes by both tree crown and trunk, B_1-B_4 are coefficients of the tree deflection equation, which are the same to A_1-A_4 in Eq. (2).

Regarding the boundary condition at the treetop (z=0) is the free end, Eq. (4) can be simplified as:

$$u_1(z)=\frac{1}{z}\left[A_1J_2\left(2\sqrt{\lambda_1 z}\right)+A_3J_2\left(2i\sqrt{\lambda_1 z}\right)\right] \qquad 0\leq z<l \quad (5)$$

According to the boundary conditions at the tree base (z=h) and the continuity conditions at the splitting points of two segments, following constraints are determined: $u_1(l)=u_2(l)$, $u_1'(l)=u_2'(l)$, $u_1''(l)=u_2''(l)$, $u_1'''(l)=u_2'''(l)$, $u_2(h)=0$, and $Ku_2'(h)+EI(h)u_2''(h)=0$. Introducing the constraints into Eqs. (4-5), these six equations can be written in a matrix format:

$$\left[F\left(\lambda_1,\lambda_2\right)\right]_{6\times6}\cdot\left[A_1 \quad A_3 \quad B_1 \quad B_2 \quad B_3 \quad B_4\right]^T=0 \quad (6)$$

where $\left[F\left(\lambda_1,\lambda_2\right)\right]_{6\times6}$ is the matrix that is composed of the eigenfrequency (ω). The orders of eigenfrequency and the corresponding vibration mode are calculated by solving the equation: the determinant of matric $\left|F(\lambda_1,\lambda_2)\right|=0$.

2.2 Dynamic response of trees

Dynamic response of trees subject to an air blast loading is calculated using a modified multi-degree-of-freedom tree swaying model [21]. To calculate the air blast loading, the size of tree crown here refers to its real frontal area distribution, which is different from the simplification in the eigenfrequency prediction mode. The tree beam is divided into a set of segments and the tree deflection is calculated using linear modal analysis. According to numerical works performed by Sellier et al. (2008)[22] and Pivato et al. (2014) [23], for trees with a slender shape, the contribution of the first vibration mode is far ahead of the others. The present work only used the first vibration mode and the corresponding eigenfrequency to calculate the tree response. Furthermore, the modelling of the air blast loading accounts for the large tree deflection and wind-tree relative motion through regarding the beam velocity and geometric nonlinearities led by the inclination of beam segments (θ_i) (Fig. 2). With respect to the large tree deflection, the impact of eccentric gravity is also involved in the model. Considering that damaged trees often fall in the direction of landslide motion and have little time to sway, the maximum response is suggested to be reached before the damping forces act [10]. The impact of damping is therefore neglected. Equations for tree motion and the air blast loading are expressed as:

$$m\frac{\partial^2 y}{\partial t^2}+ky=\int_0^h F_i\phi\mathrm{d}s+\int_0^h G_i\phi\mathrm{d}s \quad (7)$$

$$F_i=0.5\rho C_{\mathrm{d}}A_{\mathrm{f}}\left|v\cos\theta_i-\frac{\partial y}{\partial t}\cos\theta_i\right|\left(v\cos\theta_i-\frac{\partial y}{\partial t}\cos\theta_i\right)\cos\theta_i \quad (8)$$

$$G_i=m_ig\cdot\sin\theta_i\cdot\cos\theta_i \quad (9)$$

where ϕ, w, $m = \int_0^h \overline{m}\phi^2 \mathrm{d}s$, $k = 4\pi^2 m\omega^2$ represent the first mode shape, the first eigenfrequency, modal mass and stiffness, respectively. $\overline{m}$ is the mass distribution, F_i and G_i represent the air blast loading and eccentric gravity acting on the ith beam segment, h is the tree height, C_d is the drag efficient, A_f is the frontal area, ρ and v are the density and velocity of the air blast, respectively.

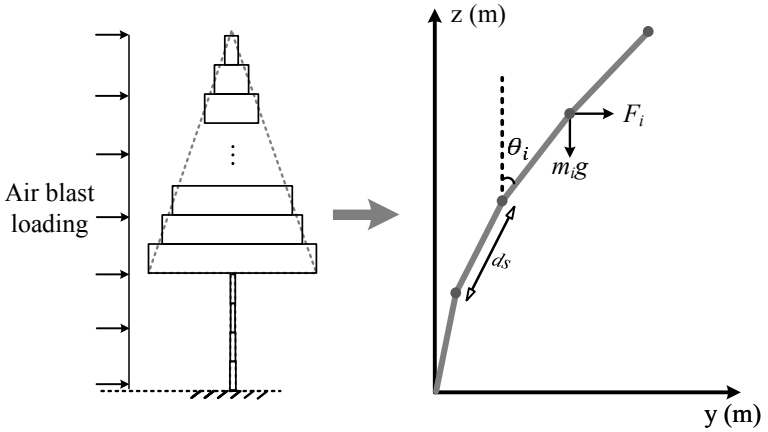

Fig. 2 Modeling the tree as a multi-degree-of-freedom flexible beam to calculate the dynamic response of trees subjected to an air blast.

In this study, the velocity of landslide-induced air blasts is characterized as a sine wave impulse with a short duration t_0:

$$v = v_{\max}\sqrt{\sin \varpi t} \tag{10}$$

where $v_{\max}$ represents the maximum air blast velocity and ϖ is treated as the circular frequency of the air blast loading $\varpi = \pi / t_0$ (wind force is linked to the square of its velocity). The dynamic response and deformation of trees subject to an air blast loading are determined by introducing the wind velocity (according to Eq. 10) into Eqs. 7-9, and then solving the tree motion equations using the central finite-difference scheme [21].

2.3 Tree breakage conditions

The present work involves two common failure modes caused by powerful air blasts: bending and overturning [14].

For the bending failure, tree breakage will occur when the maximum bending stress ($\sigma_{\max}$) reaches the bending strength (σ_{crit}):

$$\sigma_{\max} = \left[\frac{M(t,z)\cdot d(z)/2}{I(z)}\right]_{\max} \geq \sigma_{\mathrm{crit}} \tag{11}$$

where $M(t,z)$ is the bending moment, which is calculated at different positions during the air blast loading:

$$M(t,z) = EI(z)\frac{\mathrm{d}\theta}{\mathrm{d}s} \tag{12}$$

where θ represents the inclination between the beam segment with the vertical direction and $\frac{\mathrm{d}\theta}{\mathrm{d}s}$ is the local beam curvature.

For the cases of overturning, tree breakage will occur at the basement when the moment ($M_{\mathrm{base}}(t)$) exceeds the anchorage resistance (M_{crit}):

$$M_{\text{base}}(t) \geq M_{\text{crit}} \tag{13}$$

3 APPLICATION

We consider the problem proposed by Bartelt et al. (2018)[10] to illustrate the air blast power: a landslide-induced air blast enters a forest of tall spruce (25-30 m). The short-duration air blast has a maximum velocity of 20 m/s and lasts a few seconds with a frequency ϖ. The sliding mass stopped before entering the forests and only the air blast acted on trees.

Table 1 Model parameters used in the numerical simulations of the tree response. Parameters are derived from data contained in Kantola and Mäkelä (2004) and Bartelt et al. (2018).

Height h(m)	Crown height l(m)	Crown width w(m)	Diameter at trunk base D(m)	Wood density ρ_2 (kg/m^3)	Branch mass m(kg)	Drag coefficient C_d	Elastic modulus E(GPa)
27	18	5	0.4	480	540	0.4	10

Using the tree-related parameters shown in Table 1, we set the crown mass of a single tree to be 540 kg. The crown is assumed to have a cone shape with a length of 18 m ($\frac{2}{3}h$) and a width of 5 m. Neild and Wood (1999) [19] performed many in-situ measurements on spruce anchorage stiffness (K), showing a large value variation of 80-1200 kN·m. In this study, K values of 100-1200 kN·m are applied in the eigenfrequency calculation.

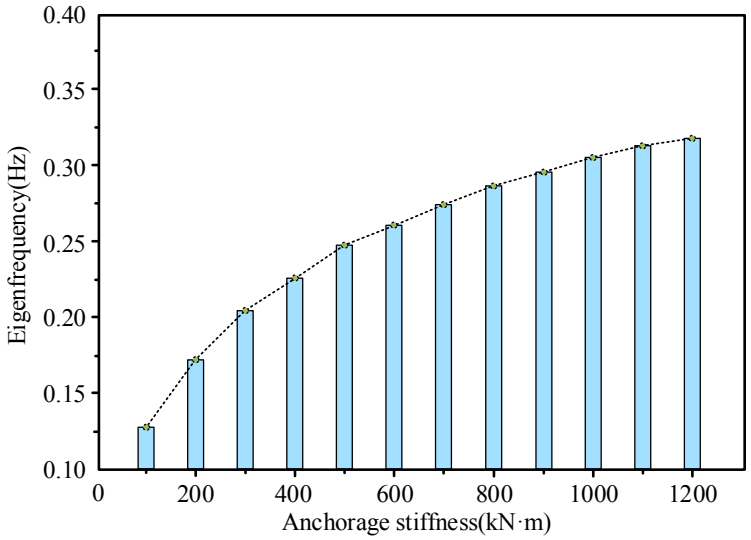

Fig. 3 Impact of anchorage stiffness on the tree eigenfrequency.

The eigenfrequency ranging from 0.13 Hz (K=100 kN·m) to 0.32 Hz (K=1200 kN·m) is calculated using the above parameters (Fig. 3), which is basically consistent with measurements performed by Jonsson et al. (2007)[24]. The good agreement between the calculated eigenfrequency and the measurement validates the proposed eigenfrequency prediction method. Notably, though the tree eigenfrequency varies significantly with the anchorage stiffness, the calculated values are always in the same order of magnitude with the air blast frequency, necessitating further research on the potential effect of resonance.

To investigate the potential dynamic magnification effect on tree deformation, we designed cases using the tree eigenfrequency of 0.26 Hz (K=600 kN·m) and the associated vibration mode. We character this effect using the ratio of the maximum dynamic deformation ($u_{\text{d,max}}$) to the static deformation (u_{sta}):

$$D = \frac{u_{\mathrm{d,max}}(\beta)}{u_{\mathrm{sta}}} = \frac{u_{\mathrm{d,max}}(\beta)}{\int_0^h F_{\mathrm{s,max}} \phi \mathrm{d}s / k} = \frac{u_{\mathrm{d,max}}(\beta)}{\int_0^h \rho C_{\mathrm{d}} A_{\mathrm{f}} v_{\mathrm{max}}^2 \phi \mathrm{d}s / k} \tag{14}$$

where $F_{\mathrm{s,max}}$ represents the maximum static wind force and $\beta = \dfrac{\varpi}{\omega}$ is the ratio between the air blast frequency (ϖ) and the tree eigenfrequency (ω). Regarding that dust mixed in the air blast would increase the fluid density, $\rho = 5\mathrm{kg/m^3}$ is utilized here [11]. In this case, the static tree deformation u_{sta} is calculated to be 9.8 m.

Fig. 4 shows the impact of dynamic magnification on tree deformation. Consider first an air blast duration of 1.6 s ($\beta = 1.2$), the maximum dynamic displacement $u_{\mathrm{d,max}}$ reaches 10.7 m, corresponding to the magnification factor D of 1.09. The air blast frequency is higher than that of trees, thus the maximum deformation reaches after the loading time. For a longer air blast lasting 3.2 s ($\beta = 0.6$), the magnification factor D is calculated to be 1.34, a high value. The maximum tree displacement happens during the air blast loading. In this scenario, an air blast with a velocity of 20 m/s can cause similar tree breakage as a long-duration wind travels at 25 m/s. Although the large tree deflection (tree inclination) decreases the wind load acting on trees, the impulse air blast will increase the risk of tree breakage because of the dynamic magnification effect.

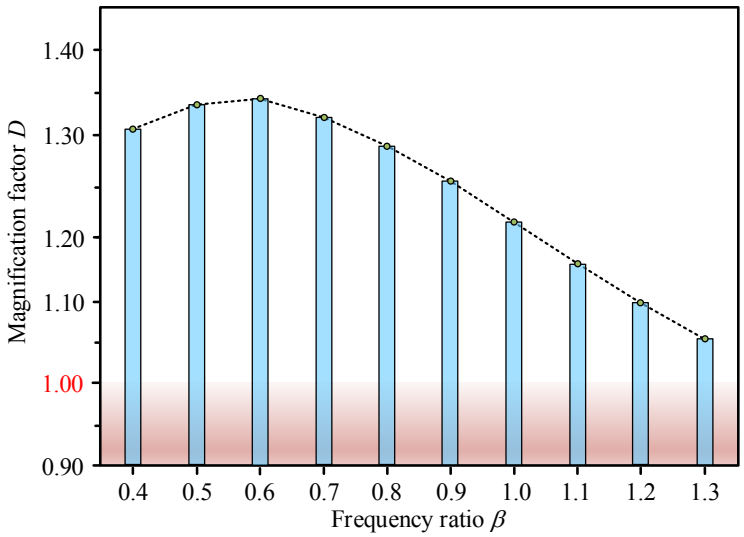

Fig. 4 Magnification factor change with various frequency ratios.

Using the proposed model, further simulations were conducted on the air blast-induced tree breakage. The air blast is assumed to have a maximum velocity of 20 m/s and lasts 3.2 s. In this case, the maximum bending stress is calculated to be 35 Mpa, located at 9 m height (crown base), while the maximum moment is identified at the tree base with a value of 192 kNm . In natural forests, it is known that the bending strength and anchorage resistance of trees depend heavily on tree species, soil characteristics and climates, etc. In-situ measurements performed by Peltola et al. (1999) [13] indicated that the bending stress to destroy mature trees should exceed a minimum value of 30 Mpa, and anchorage resistance of mature spruces could reach up to 100-400 kN·m. Therefore, bending and overturning failure will both likely happen for the case performed in this study.

4 DISCUSSION

Evaluation of air blast hazards is an important issue of landslide risk assessment in mountainous regions. Compared with existing models, one improvement of our model is to involve the impact of anchorage and treat trees as beams with a variable cross-section. This improvement allows trees to sway as their natural vibration and make the bending failure more realistic. The failure position can be simulated using the proposed model. In previous models that describe the air blast-tree interaction, trees are modelled as beams with a constant diameter [11], and thus the maximum bending stress always reaches at the tree base. This failure feature is greatly different from the field observations.

Another improvement of the proposed model is to involve the large tree deflection. A comparative analysis is designed to investigate its impact on tree response. We simplified the tree motion equation of Eq. 7 without accounting for the large tree deflection. The simplified model is similar to that proposed by Bartelt et al. (2018) [10]:

$$m\frac{\partial^2 y}{\partial t^2}+ky=\int_0^h 0.5\rho C_{\mathrm{d}}A_{\mathrm{f}}v_{\max}^2\phi \mathrm{d}s\cdot\sin\varpi t=\int_0^h F_{\mathrm{s,max}}\phi \mathrm{d}s\cdot\sin\varpi t \tag{15}$$

The displacement at the tree top can be written as:

$$\begin{cases} u(t)=\dfrac{\int_0^h F_{\mathrm{s,max}}\phi \mathrm{d}s}{k}\dfrac{1}{1-\beta^2}(\sin\varpi t-\beta\sin\omega t) & 0\le t\le t_0 \\ u(t)=\dfrac{u'(t_0)}{\omega}\sin\omega(t-t_0)+u(t_0)\cos\omega(t-t_0) & t>t_0 \end{cases} \tag{16}$$

The magnification factor D for both scenarios can be expressed as:

$$\begin{cases} D=\dfrac{1}{1-\beta^2}\left[\sin\left(\dfrac{2\pi\beta}{\beta+1}\right)-\beta\sin\dfrac{2\pi}{\beta+1}\right] & \beta\le 1 \\ D=\dfrac{2\beta}{\beta^2-1}\cos\dfrac{\pi}{2\beta} & \beta>1 \end{cases} \tag{17}$$

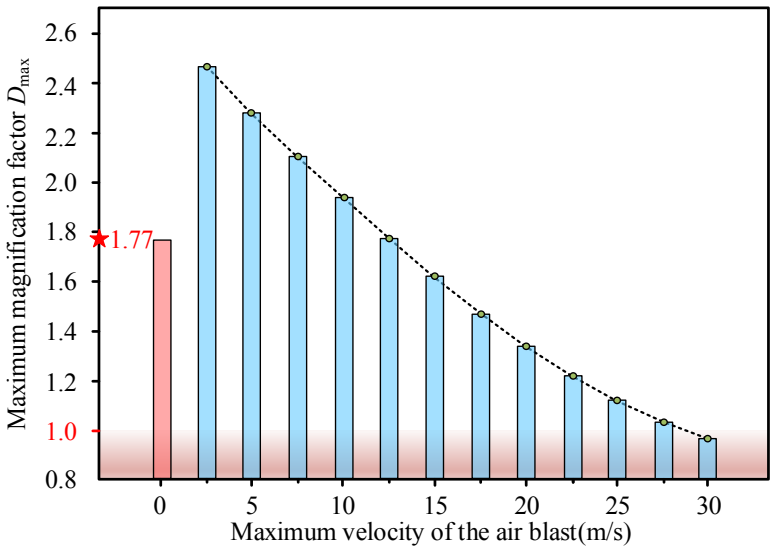

Fig. 5 Impact of large tree deflection on the maximum magnification factor $D_{\max}$. The red star represents the $D_{\max}$ calculated from Eq. 17. The red bar represents the $D_{\max}$ corresponding to the scenario with a very low air blast velocity (maximum velocity of 0.1m/s) and the eccentric gravity is not considered.

The impact of large tree deflection on the magnification effect is shown in Fig. 5. In the case of a very low wind velocity (maximum velocity of 0.1m/s) and in the absence of eccen-

tric gravity, the D_{max} value is calculated to be 1.77, which is in agreement with the analytical solution from Eq. 17. This scenario ignores the impact of large tree deflection. The tree displacement is small when subjected to such a weak air blast loading, and the comparison result validates the proposed model. Further calculations accounting for the impact of large tree deflection show different results. In the cases of a low wind velocity, the eccentric gravity is significantly influential, leading to a rather high magnification factor (>2). Nevertheless, D_{max} greatly decreases in the cases of a larger wind velocity. The dynamic response and eccentric gravity amplify the tree deflection, but the tree inclination reduces the frontal area and the associated air blast loading. This special mechanism is rarely considered in previous air blast risk assessments. The modelled tree deflection subjected to a strong air blast might be overestimated without accounting for the large tree deflection.

The mechanical response and failure of trees subject to a powerful air blast are complex, depending on the biometric characteristics of trees. Some biomass changes can be represented through modifying parameters in the proposed model. For example, for leafless trees, air blasts only act on the branch, leading to a smaller wind load [25]. A small drag efficient C_d will provide better performance. Due to the shielding effect of forests, single trees are always subject to a larger wind loading than trees in dense forest stand [11]. A reduction of the frontal area A_f is needed in such a condition. Additionally, the anchorage characteristic is also influential as it greatly contributes to the tree eigenfrequency and the likely failure mode. For now, though many efforts have been paid to mechanical properties of trunks, little information is available about the anchorage stiffness and resistance of trees. A reliable test value of anchorage resistance and bending strength is of utility to help the tree failure prediction and clarify which failure mode will occur. In the future, regional databases for the mechanical and biometric properties of trees are suggested to be established. This would provide reliable information for geologists during the risk assessment of landslide-induced air blasts.

5 CONCLUSIONS

Landslide-induced air blasts are short-duration impulses and can cause damage far beyond the sliding mass. Tree breakage in situ provides the opportunity to quantify the air blast power. In this study, we proposed a framework to assess the air blast danger using the tree breakage information, including the eigenfrequency prediction method, tree motion equations and breakage conditions. Trees are modelled as a flexible variable cross-section beam hinged at ground using elastic support. The impacts of anchorage and large tree deflection are involved in the model. We draw several conclusions from the analysis.

Though the anchorage property is greatly influential to the tree eigenfrequency, the tree eigenfrequency is always in the same order of magnitude as the air blast frequency. The associated dynamic response amplifies the tree deflection and leads to a higher risk of tree breakage. Short-duration air blasts travelling at 20 m/s can cause similar damage as a long-duration wind moves at 25 m/s. Notably, this magnification effect results from dynamic loading and eccentric gravity is significant in a weak wind case, while large tree deflection (tree inclination) caused by powerful air blasts would weaken the effect. Additionally, bending and overturning are two likely failure modes for trees, but what kind of failure will occur for a specific forest depends heavily on tree properties. In the future, more measurements are needed to be conducted on the mechanical and biometric properties of trees, which will help the prediction of air blast danger.

REFERENCES

[1] De Blasio FV, Crosta GB (2015) Fragmentation and boosting of rock falls and rock avalanches. Geophysical Research Letters, 42, 8463-8470.

[2] Yin YP (2014) Vertical acceleration effect on landsides triggered by the Wenchuan earthquake, China. Environmental Earth Sciences, 71, 4703-4714.

[3] Penna IM, Hermanns RL, Nicolet P, Morken OA, Jaboyedoff M (2021) Airblasts caused by large slope collapses. Geological Society of America Bulletin, 133, 939-948.

[4] Bartelt P, Buser O, Vera Valero C, Bühler Y (2016) Configurational energy and the formation of mixed flowing/powder snow and ice avalanches. Annals of Glaciology, 57(71), 179-188.

[5] Zhuang Y, Xu Q, Xing AG (2019) Numerical investigation of the air blast generated by the Wenjia valley rock avalanche in Mianzhu, Sichuan, China. Landslides, 16, 2499-2508.

[6] Zhuang Y, Xu Q, Xing AG, Bilal M, Gnyawali KR (2022a) Catastrophic air blasts triggered by large ice/rock avalanches, Landslides. Doi: 10.1007/s10346-022-01967-8.

[7] Sukhanov G (1982) The mechanism of avalanche air blast formation as derived from field measurements, Data Glaciology Student, 44, 94-98.

[8] Caviezel A, Margreth S, Ivanova K, Sovilla B, Bartelt P (2021) Powder snow impact of tall vibrating structures. Eccomas Proceedia Compdyn, 5318-5330.

[9] Yin YP, Xing AG (2012) Aerodynamic modeling of the yigong gigantic rock slide-debris avalanche, Tibet, China. Bulletin of Engineering Geology and the Environment, 71, 149-160.

[10] Bartelt P, Bebi P, Feistl T, Buser O, Caviezel A (2018) Dynamic magnification factors for tree blow-down by powder snow avalanche air blasts. Natural Hazards Earth System Sciences, 18, 759-764.

[11] Feistl T, Bebi P, Christen M, Margreth S, Diefenbach L, Bartelt P (2015) Forest damage and snow avalanche flow regime. Natural Hazards and Earth System Sciences, 15, 1275-1288.

[12] Fujita K, Inoue H, Izumi T, Yamaguchi S, Sadakane A, Sunako S, Nishimura K, Immerzeel WW, Shea JM, Kayastha RB, Sawagaki T, Breashears DF, Yagi H, Sakai A (2017) Anomalous winter-snow-amplified earthquake-induced disaster of the 2015 Langtang avalanche in Nepal, Natural Hazards Earth System Sciences. 17, 749-764.

[13] Peltola H, Kellomäki S, Väisänen H, Ikonen V (1999) A mechanistic model for assessing the risk of wind and snow damage to single trees and stands of scots pine, norway spruce, and birch. Canadian Journal of Forest Research, 29, 647-661.

[14] Gardiner B, Peltola H, Kellomäki S (2000) Comparison of two models for predicting the critical wind speeds required to damage coniferous trees. Ecological Modelling, 129, 1-23.

[15] Jonsson MJ, Foetzki A, Kalberer M, Lundström T, Ammann W, Stöckli V (2006) Root-soil rotation stiffness of norway spruce (Picea abies (L.) Karst) growing on subalpine forested slopes, Plant Soil, 285, 267-277.

[16] Nicoll BC, Gardiner BA, Rayner B, Peace AJ (2006) Anchorage of coniferous trees in relation to species, soil type, and rooting depth. Canadian Journal of Forest Research, 36, 1871-1883.

[17] Bartelt P, Stöckli V (2001) The influence of tree and branch fracture, overturning and debris entrainment on snow avalanche flow. Annals of Glaciology, 32, 209-216.

[18] Grigoryan S, Urubayev N, Nekrasov I (1982) Experimental investigation of an avalanche air blast. Data Glaciology Student, 44, 87-93.

[19] Neild AS, Wood CJ (1999) Estimating stem and root-anchorage flexibility in trees. Tree Physiology, 19, 141-151.

[20] Keshmiri A, Wu N, Wang Q (2018) Free Vibration Analysis of a Nonlinearly Tapered Cone Beam by Adomian Decomposition Method. International Journal of Structural Stability and Dynamics, 18(7), 1850101.

[21] Zhuang Y, Xing AG, Jiang YH, Sun Q, Yan JK, Zhang YB (2022b) Typhoon, rainfall and trees jointly cause landslides in coastal regions. Engineering Geology, 298, 106561.

[22] Sellier D, Brunet Y, Fourcaud T (2008) A numerical model of tree aerodynamic response to a turbulent airflow. Forestry, 81(3), 279-297.

[23] Pivato D, Dupont S, Brunet Y (2014) A simple tree swaying model for forest motion in windstorm conditions. Trees, 28, 281-293.

[24] Jonsson MJ, Foetzki A, Kalberer M, Lundström T, Ammann W, Stöckli V (2006) Root-soil rotation stiffness of norway spruce (Picea abies (L.) Karst) growing on subalpine forested slopes. Plant Soil, 285, 267-277.

[25] Schelhaas MJ, Kramer K, Peltola H, Werf DC, Wijdeven SMJ (2007) Introducing tree interactions in wind damage simulation. Ecological Modelling, 207(2-4), 197-209.